Proceedings of the 12th International Conference on
Aluminium Alloys, September 5-9, 2010, Yokohama, Japan

pp. 1165-1172

The Effect of Non-Linear Deformation History on Microstructure and Recrystallization in Hot Worked Aluminium

B.P. Wynne[1], M. Lopez-Pedrosa[1], O. Hernandez-Silva[1], and W.M. Rainforth[1]

[1]Institute for Microstructural and Mechanical Process Engineering: The University of Sheffield, Mappin Street, Sheffield, S1 3JD, UK.

The effects of non-linear strain paths on the deformation microstructure evolution and subsequent static recrystallization in hot worked AA5052 have been studied using high resolution electron backscatter diffraction. It is concluded that instantaneous deformation mode determines the orientation of deformation induced features such as microbands, whilst a non-linear strain path history influences the range of misorientation angle in the material through the dissociation of previously formed microbands and the formation of new microbands at the new straining condition, leading to a lower level of misorientation angle. This in turn has a dramatic influence on recrystallization response with a much larger grain size produced for all non-linear strain path conditions for the same level of total strain.

Keywords: *Hot working, Strain path, recrystallization, electron backscatter diffraction, AA5052.*

1. Introduction

Many industrial thermomechanical processing routes of aluminium alloys subject the material to complex non-linear deformation histories, with changes in strain rate, temperature and strain path, i.e. changes in the relative contributions of each of the strain components, as deformation proceeds. This is generally manifested in two distinct ways: 1. discontinuous strain path changes which generally involve a relative large strain path angle change between deformation passes such as that involved in a cogging or cross rolling operation, and 2. continuous strain path changes which involve a gradual change in the applied strain tensor during the deformation step due to geometric constraints or interfacial friction conditions such as those involved in closed die forging or slab rolling. Microstructure predictions models, however, are often found to be inadequate under such conditions with the error increasing the further the process deviates from linearity [1,2]. Sellars [3] suggests two reasons for this discrepancy: first, currently most microstructure models are described in terms of equivalent stresses and strains, so that much of the information provided by computational plasticity simulations cannot be fully utilized, and second, the testing methods (e.g. axisymmetric compression, plane strain compression, torsion testing) used to obtain experimental data to calibrate the microstructure prediction equations are linear unidirectional tests. With the second point in mind the objective of this paper is to examine the effect of a variety of strain path changes on the deformation microstructure and subsequent static recrystallization behaviour of aluminium alloy AA5052 deformed under hot working conditions. To achieve this task the arbitrary strain path test machine (ASP) at the University of Sheffield has been used. This machine is capable of applying torsion (forward and reverse) and axisymmetric (tension and compression) deformation under well controlled conditions either sequentially or concurrently at strain rates and temperatures observed in industrial operations. The specific aim being to gain an insight into what are the strain path sensitive variables that need to be incorporated into to the current models to gain better microstructure predictions under non-linear strain path histories. In this case the microstructure has been investigated using high resolution electron backscattered diffraction (EBSD) and deformation microstructure features such as microbands and misorientation distribution have been investigated and described as a function of strain path in order to correlate those features with variations observed in recrystallization response.

2. Experimental Material and Procedure

The material used in this study was the commercial aluminium alloy AA5052 supplied by Alcan International in the form of 30 mm thick hot rolled transfer bar. The material was recrystallized containing equiaxed grains with an average grain size of 67 µm and a weak cube texture. The test specimens of 10mm diameter and 20mm gauge length were machined such that the longitudinal direction (Z) was perpendicular to the as-received rolling direction. Seven strain path tests in deformation steps of either forward torsion (ForTor), reverse torsion (RevTor), tension (Ten) or compression (Com), outlined in Table 1, were undertaken at a temperature of 300°C and a strain rate of $1s^{-1}$. Note all strains in Table 1 are in equivalent von Mises strain.

Table 1. Strain path experiments undertaken.

Test	Step 1/Strain	Step 2/Strain	Step 3/Strain	Total Strain
1	ForTor (0.25)	-	-	0.25
2	ForTor (0.25)	ForTor (0.25)		0.50
3	ForTor (0.25)	RevTor (0.25)		0.50
4	ForTor (0.25)	RevTor (0.05)		0.30
5	ForTor (0.25)	ForTor (0.25)	RevTor (0.05)	0.55
6	ForTor (0.25)	Ten (0.25)		0.50
7	ForTor (0.25)	Com (0.25)		0.50

For all the experiments after each intermediate deformation step the rotational torque and axisymmetric load was dropped to zero before the next step was undertaken. The time between deformation steps was less than 1 second. After the final deformation step the specimens were immediately quenched using a water spray. Subsequent static recrystallization experiments were then performed on slices of the gauge length at 400°C in a salt bath for all deformation conditions for 60 minutes.

Specimens for EBSD analysis of microstructure were sectioned parallel to the longitudinal direction of the torsion specimens and then mechanically ground and polished using 3- and 1-µm diamond pastes to 0.8 of the radius and subsequently electropolished in 30% nitric acid in methanol at a temperature of approximately -15°C using 12V and 1 mA for 120 seconds. The EBSD data was acquired in the radius (R) plane, i.e. the plane containing the Z and rotation (θ) specimen directions, using an FEI Sirion FEGSEM equipped with a HKL Nordlys CCD camera controlled by HKL Channel 5 acquisition software. The EBSD acquisition data were collected with a step size of 0.25µm. The efficiency of the indexing of the EBSD patterns was of the order of 90–95%. Subsequent data analysis was performed using HKL Channel 5 software and VMAP V.8 kindly provided by Professor F.J. Humphreys, The University of Manchester [4].

For Tests 2 and 3 a detailed analysis of the macroscopic orientation of deformation induced microbands with respect to the maximum principal stress and strain directions was undertaken. For the ForTor/ForTor case the maximum principal stress lies at +45° (Fig.1a) to the longitudinal direction. Microbands rotated anticlockwise from these directions were considered to be positive, whilst a clockwise rotation was considered negative. For the ForTor/RevTor case, microbands were quantified with respect to the maximum principal stress of the final deformation pass, i.e. the maximum principal stress lies at -45° to longitudinal direction (Fig. 1b). To maintain the same relationship between microband angle and forward torsion microbands, reverse torsion microbands rotated anticlockwise from the tensile stress axis were considered to be negative, whilst a clockwise rotation was considered positive. The principal strain direction was calculated using Eq. 1 [5].

$$\delta = 90 - \frac{1}{2} tan^{-1} \frac{2}{\gamma} \tag{1}$$

Figure 2 shows schematically the principal strain directions for tests 2 and 3. It should be noted that for the calculation of the principal strain direction in the case of ForTor/RevTor it was assumed that there was no previous strain history prior to reverse torsion and the angle was calculated using a strain of 0.25. The same angle convention as described above was used to define the orientation of microbands relative to the principal strain direction.

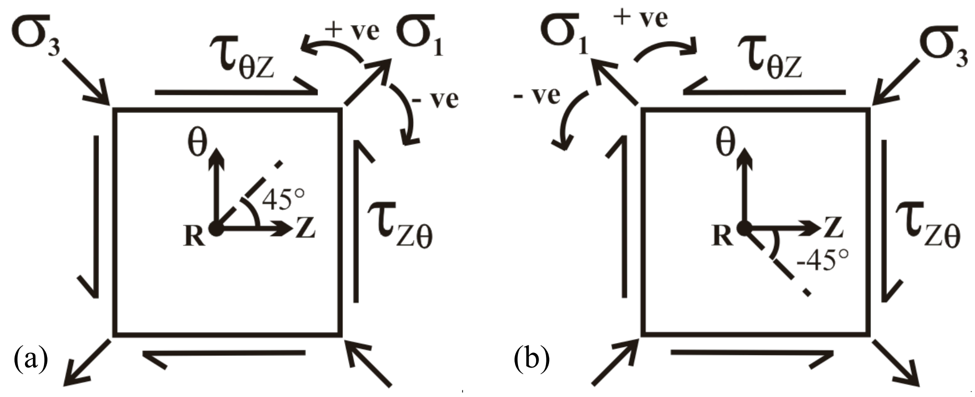

Figure 1. Definition of principal stress direction for forward (a) and reverse (b) torsion. +ve and –ve refer to the definition of microband angle

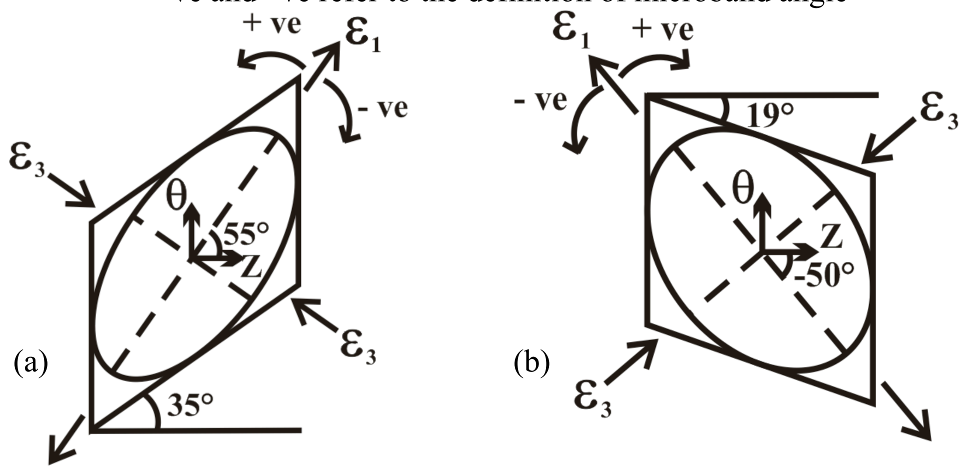

Figure 2. Definition of principal strain direction for (a) ForTor/ForTor and (b) ForTor/RevTor.

For investigation of the amount of substructure/stored energy within individual grains following the various strain path tests, the mean orientation of each grain and the deviation from the mean for each point in the grain was calculated following the approach developed by Glez and Driver [6]. This also enabled recrystallized grains to be identified, i.e. if the average deviation from the mean for each data point within the grain was below a certain threshold (1.2° in this case) then the grain was considered to be recrystallized.

3. Results and discussion

For tests 2 and 3 microbands were observed in 63 grains for ForTor/ForTor and 60 grains for ForTor/RevTor. The analysed grains mostly displayed either one or two sets of microbands with a few grains exhibiting three sets of microbands. An example grain of the ForTor/RevTor material is shown in Fig. 3. Like all grains observed the grain has returned to its original equiaxed shape. The microstructure consists of a parallel arrangement of one set of microbands with a mean alternating misorientation angle of 1.3º and mean spacing of 2.0 μm orientated at -34º to the principal stress direction and -39º to the principal strain direction.

The macroscopic orientations of all microbands measured in relationship to the principal directions are shown in Fig. 4. For ForTor/ForTor (Fig.4a) there appears to be two distinct spatial groupings, i) parallel to the maximum shear stress direction (+45° with respect to the principal stress direction) with very little spread and ii) clustered around -10° to -30°. For the ForTor/RevTor condition (Fig. 4b) microband angles have become significantly more spread, with a slight clustering around ±35° with respect to the principal stress direction of the reverse torsion. When the ForTor/ForTor microbands are related to the principal strain direction (Fig. 4c) positive microband angles tend to cluster strongly at around +35º and negative microband angles lie at around -40º to -30º, similar to that observed in rolling where microbands are orientated approximately ±35º to the rolling direction [7,8]. But again only slight clustering could be observed for the ForTor/RevTor condition (Fig. 4d).

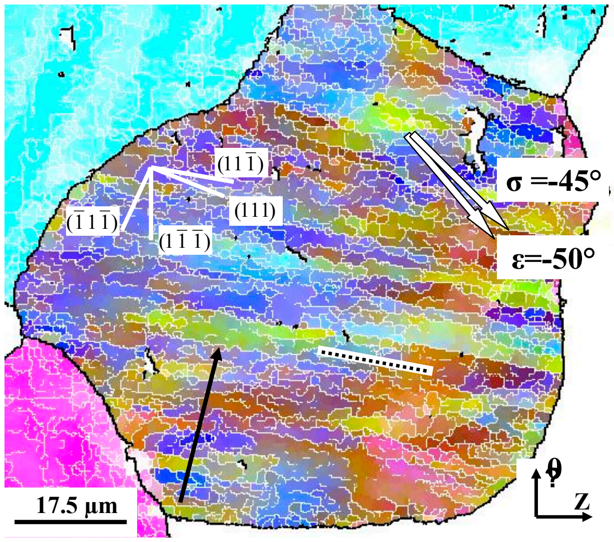

Figure 3. Relative Euler angle map for a grain of ForTor/RevTor. Boundaries superimposed have misorientation angles 0.5º (thin white) and 10º (thick black). Dotted line represents set of microband orientation and solid white lines are {111} traces.

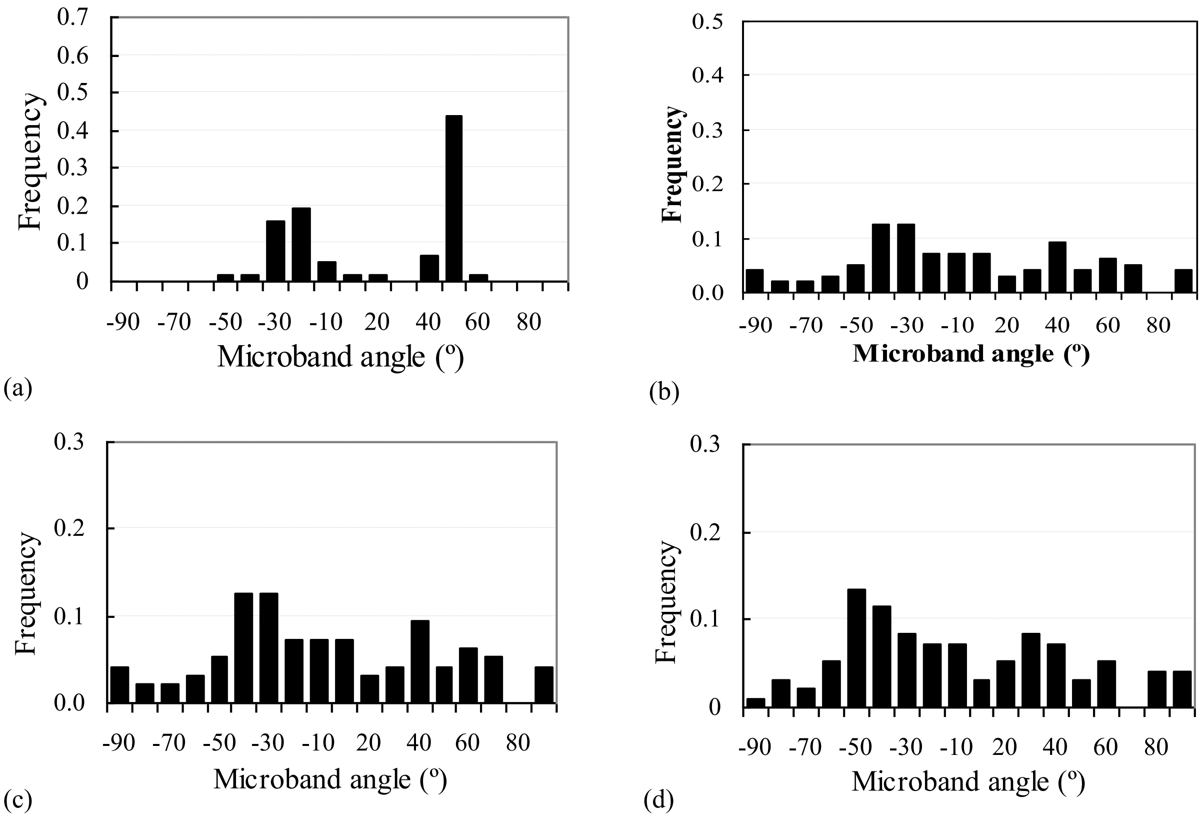

Figure 4. Histograms showing the angle between microbands and the maximum principal stress directions for (a) ForTor/ForTor & (c) ForTor/RevTor and the maximum principal strain directions for (b) ForTor/ForTor & (d) ForTor/RevTor.

The data presented here also corresponds closely to the data of Hughes and Hansen [9], for room temperature deformed nickel deformed to slightly lower strain levels. This would suggest that like other deformation modes the microband angle distribution for torsion is very similar for both hot and cold deformation and materials of similar stacking fault energy. In comparison, when the strain path is reversed halfway through the deformation sequence a significant spread in microband angle is produced. This observation corresponds closely with the results reported by Zhu and Sellars [10] following tension/compression testing of high purity Al-3%Mg who found a bimodal distribution of microband angles following reversed deformation. They suggested that the reverse deformation did not change the angle of microbands in the first deformation but dissociated the original ones and made new ones at angles dependent on the new deformation mode. This also appears to be happening in the current case where the new peaks of microband angle look to be emerging at ±35° to the principal axes of the reverse deformation and the total level of low angle boundary misorientation within the material is considerably reduced compared to the forward material (Fig 5.). This suggests that the instantaneous deformation mode determines the orientation of any new microbands formed whilst the strain path history influences misorientation angle within the material.

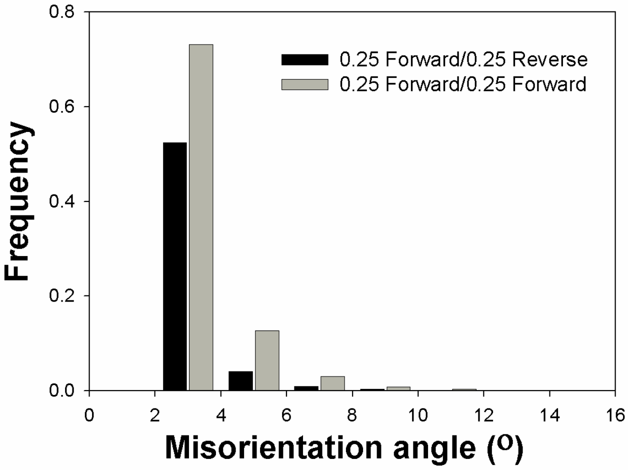

Figure 5. Comparison of ForTor/ForTor and ForTor/Rev misorientation histograms for low-angle boundaries. The cutoff angle was defined as 2°

A more detailed analysis of misorientation distribution is given in Fig. 6 which shows the misorientation within the grain from the mean orientation of the grain. Figs. 6 a and c show the deviation from the mean for each point within the grain, whilst Figs. 6 b and d shows the average deviation from the mean for each grain. For ForTor/ForTor (Figs. 6 a and b) the majority of grains show a relatively high deviation from the mean indicating that all grains contain significant stored energy. In comparison the ForTor/RevTor case presents a bimodal distribution with about 50% of the grains having significant deviation from the mean, whilst the other half have average deviations less than 1.2°, i.e. indicating they are virtually strain free. This variation in stored energy is borne out in the recrystallization response of these two materials shown for the 60 minutes annealed condition in Fig. 7. For ForTor/ForTor (Fig. 7a) the material is completely recrystallized with a fine equiaxed grain structure. In comparison for ForTor/RevTor (Fig. 7b) there is only a small amount of recrystallization which is confirmed by the grain size measurements with no significant change in grains size between the deformed material (63 μm) and the annealed material (76 μm). The IPF map also highlights that substructure is still present within ForTor/RevTor confirming no recrystallization has taken place in those areas. This strong dependence on strain path of static recrystallization response shown here is similar to that found by Zhu and Sellars [11] for a commercial purity Al-2%Mg deformed in tension followed by compression to a total strain of 0.28. In that work the time for 50% recrystallization was found to be 325 times greater for the reversed condition than straight tension. They concluded the reduction in heterogeneity of the dislocation substructure on reversing the strain played the major role in retarding recrystallization by hindering the occurrence of nucleation as the non-linear strain path produced a recrystallized grain size of 460 μm compared to 75 μm for the linear strain path. The major affect of the reduction in stored energy (i.e. misorientation)

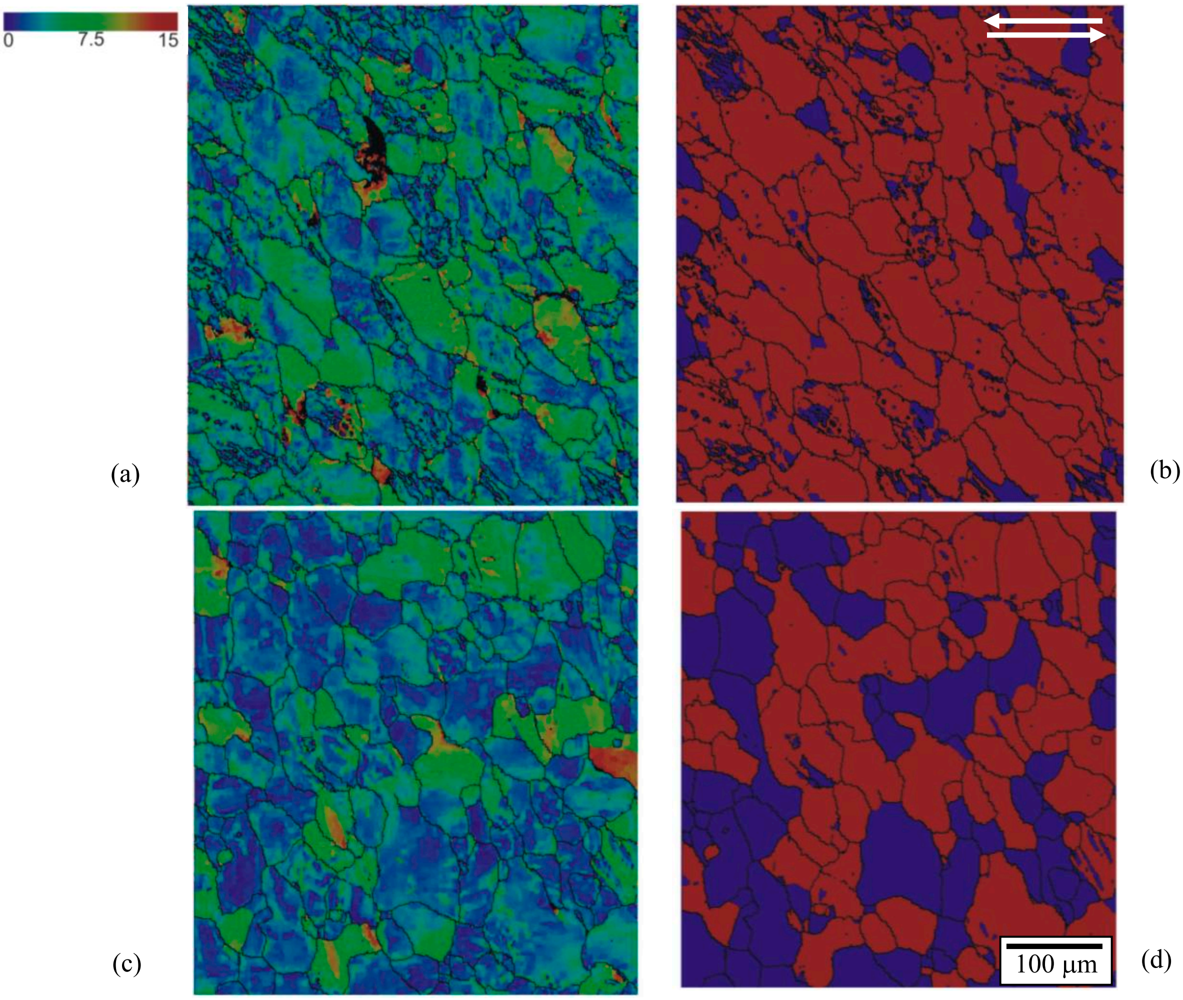

Figure 6. Deviation from the mean orientation for each point within a grain for (a) ForTor/ForTor and (c) ForTor/RevTor and average deviation from the mean orientation for each grain for (b) ForTor/ForTor and (d) ForTor/RevTor. Blue grains have average deviation from the mean less than 1.2° and red grains greater than 1.2°.

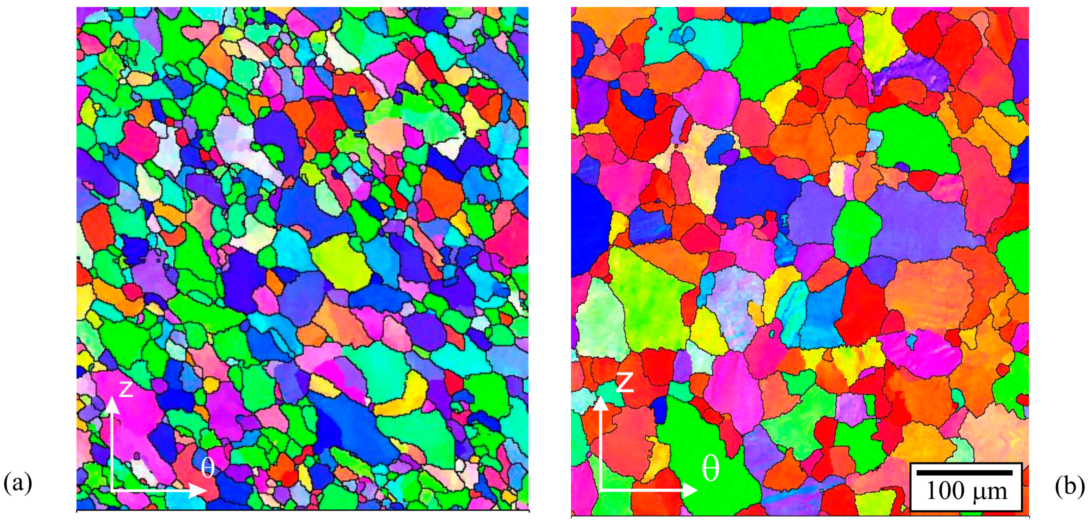

Figure 7. EBSD IPF maps of the (a) ForTor/ForTor and (b) ForTor/RevTor annealed at 400°C for 60 minutes

was only to proportionally slow the growth rate. Currently our dataset is incomplete but preliminary data suggests that this idea has merit.

The effect of the more complicated deformation conditions on the recrystallized grain size is outlined in Table 2. As expected with increasing linear strain, i.e. Test 1 to Test 2 the recrystallized grain size decreases. More interestingly, however, the data shows that in all non-linear tests the grain size is much greater than the linear condition for the same amount of strain. Moreover, the effect of a small reversal (Tests 4 and 5) is just as significant as a large reversal. In hindsight this may be quite logical, as it could be envisaged that the microstructure will be in its greatest state of disorder, particularly the sights of nucleation, straight after a strain path change leading to a much different annealing response. Further work is now under way to investigate this idea further.

Table 1. Grain size of all strain paths after 60 minutes annealing

Test	Step 1/Strain	Step 2/Strain	Step 3/Strain	Total Strain	Grain Size (µm)
1	ForTor (0.25)	-	-	0.25	56
2	ForTor (0.25)	ForTor (0.25)		0.50	29
3	ForTor (0.25)	RevTor (0.25)		0.50	76
4	ForTor (0.25)	RevTor (0.05)		0.30	61
5	ForTor (0.25)	ForTor (0.25)	RevTor (0.05)	0.55	65
6	ForTor (0.25)	Ten (0.25)		0.50	78
7	ForTor (0.25)	Com (0.25)		0.50	45

Conclusions

High resolution electron backscatter diffraction and the ASP test machine has been used to study the effects of strain path change during hot working on the microstructure evolution in the commercial aluminium alloy AA5052. In terms of microbands for ForTor/ForTor they were aligned in two clusters at +45° and around -10° to -30° to the equivalent tensile axis, whilst for ForTor/RevTor they were aligned at ±35° but with significantly more spread. There is also a significant reduction in the total level of low angle boundary misorientation in the ForTor/RevTor material compared to the ForTor/ForTor material. This leads to the conclusion that the spatial alignment of deformation induced substructure, i.e. microbands and the misorientation they accommodate is strain path sensitive. We believe in this particular case microbands formed in the forward deformation have or are dissolving during the reverse deformation and any new microbands formed are related to the deformation conditions of the final strain path leading to a more chaotic microstructure with a much lower level of stored energy. This in turn has a dramatic influence on recrystallization response with a much larger grain size produced for all non-linear strain path conditions. Further work is now required to establish the full recrystallization response of the non-linear conditions in order to determine if the major effect of strain path is on retarding nucleation, growth or both.

Acknowledgements

The authors gratefully acknowledge the financial support provided by the Engineering and Physical Sciences Research Council, U.K.and the supply of experimental material by Alcan International. One author, OH, also acknowledges the National Council of Science and Technology of Mexico (CONACYT) for financial support to study in the UK.

References

[1] C.M. Sellars and B.P. Wynne: *in 25th Risø International Symposium on Materials Science: Evolution of Deformation Microstructures in 3D*, Ed. By C. Gunglach et al., (Risø National

Laboratory, Denmark, 2004), pp 117-136.
[2] A.J. McLaren. N. LeMat. J.H. Beynon & C.M. Sellars: Iron- & Steelmaking, 22, (1995), 71-73.
[3] C.M. Sellars: *in Thermomechanical Processing in Theory, Modelling and Practice [TMP]2*, Ed. by B. Hutchinson et al., (The Swedish Society for Materials Technology, 1997), pp. 35-51.
[4] Humphreys F.J., Bate P.S., Hurley P.J.: J. Micros, 201, (2001), 50–58.
[5] G. R. Canova, S. Shrivastava, J.J. Jonas. and C. G'Sell: *in Formability of Metallic Materials 2,000 AD - ASTM STP 753*, Ed. by J.R. Newby and B.A Niemeier, (ASTM International, 1982), pp. 189-210.
[6] J.C. Glez and J. Driver: J. Applied Crystallography, 34, (2001), 280-288.
[7] G.H Akbari, C.M. Sellars and J. Whiteman: Acta Mater., 45 (1997), pp. 5047-58.
[8] P.J.Hurley and F.J. Humphreys F.J.: Acta Mater., 51 (2003), pp.1087–1102.
[9] D.A. Hughes and N. Hansen: Mater Sci. Tech., 7 (1991), pp. 544-553
[10] Q. Zhu and C.M. Sellars:. Scripta. Mater., 45 (2001), pp. 41-48.
[11] Q. Zhu and C.M. Sellars: in Proc Third Internat. Conf on Recrystallization and Related Phenomena (ReX'96), Ed. By Terry R McNelley Monterey, California, 1996, p. 81.